Resource Assessment of Ocean Thermal Energy Conversion, Tidal Stream, and Ocean Current for Powering Blue Economy Applications in Puerto Rico

Zhaoqing Yang[1], Fadia Ticona Rollano[1], Gabriel García Medina[1], and Andrea Copping[1]

1. Pacific Northwest National Laboratory, 1100 Dexter Avenue North, Suite 400, Seattle, WA 98109, USA

***Keywords*—ocean current, ocean thermal energy, OTEC, Puerto Rico, tidal energy.**

I. INTRODUCTION

THE governance of Puerto Rico set the goal to transition to using 100% renewable energy for all of its power demands by 2050 [1]. To support this goal, three national laboratories collaborated on a two-year project entitled "Puerto Rico Grid Resilience and Transitions to 100% Renewable Energy" (PR100), to identify the electrical needs and renewable energy resources available in the region. Being an island territory, Puerto Rico is uniquely positioned to tap into marine energy resources to meet their renewable energy goals and enhance their coastal resilience. This study is particularly concerned with assessing Puerto Rico's energy potential from tidal streams, ocean currents, and ocean thermal gradients. Greater focus is given to the latter for ocean thermal energy conversion (OTEC) systems because it represents a bigger gap in current research. The power yields of each energy source are estimated through different numerical models, validated against in-situ measurements, and used to highlight regions with greater power potential in the context of blue economy applications.

II. METHODS

Tides, ocean currents, and thermal gradients are assessed based on different numerical models, each chosen for its ability to resolve the unique hydrodynamic characteristics of each resource.

A. Model selection and data acquisition

The hydrodynamic model chosen to assess the tidal resource is the ADvanced CIRCulation (ADCIRC) Model v53.04. The model was executed using an existing unstructured grid previously used for storm surge modelling [2]. The high resolution of the grid, with elements as fine as 30 to 100 m along Puerto Rico's coastlines, is ideal for accurately simulating tidal currents through small channels. The forcing for the Atlantic Ocean open boundary was retrieved from the LeProvost dataset through the Surface-water Modeling System (SMS) ADCIRC module for 8 tidal harmonic constituents (4 semidiurnal: M2, S2, N2, K2; 4 diurnal: K1, O1, P1, Q1). The model was used to simulate tidal conditions for the month of May 2012 with a 1-hour output interval.

The resource characterization of ocean currents and ocean thermal energy is based on open-source model results. Ocean current data was obtained from the American Seas (AmSeas) regional Navy Coastal Ocean Model (NCOM) simulations for an eight-year period from 2014 to 2021 [3]. The model uses the Navy Coupled Ocean Data Assimilation (NCODA) to assimilate verified observations in the Gulf of Mexico and Caribbean, including satellite sea surface temperature and altimetry, as well as surface and profile temperature and salinity data. AmSeas was selected to characterize the power available from ocean currents because it has sufficient grid resolution to resolve the hydrodynamic processes near island features.

Sea temperature data was obtained from the global ocean circulation model HYbrid Coordinate Ocean Model (HYCOM) from 2008 to 2021 [4]. Simulation results for this time frame corresponds to two implementations of the model: Global Ocean Forecasting System (GOFS) 3.0 and 3.1. The two versions of HYCOM were compared over their overlapping record lengths and showed little variability for the purpose of this analysis for which the records were combined using GOFS 3.0 through June 2014 and GOFS 3.1 as of July 2014. This dataset was chosen for the OTEC analysis because it provides good coverage and an adequate vertical resolution for resolving the thermocline and mid-water column temperature gradients, as well as a long data record that can be used for evaluating the influence of low frequency climate patterns such as El Niño cycles. A summary of the AmSeas and HYCOM models is shown in Table I.

TABLE I
MODEL PROPERTIES FOR AMSEAS AND HYCOM

Station ID	AmSeas	HYCOM GOFS 3.0	HYCOM GOFS 3.1
Record length	2014 –2021	2008 –2018	2014 –2021
Horizontal resolution	1/30°	1/12°	1/12°
Number of vertical levels	40	33	40

B. Equations

The ADCIRC model was evaluated by comparing water level outputs with National Oceanic and Atmospheric Administration (NOAA) historical records at the stations shown in Fig. 1. These data were used to compute commonly used error metrics including the root-mean square-error (*RMSE*), bias, and linear correlation coefficient (R) as follows

$$RMSE = \sqrt{\frac{\sum_{i=1}^{N}(P_i - M_i)^2}{N}} \tag{1}$$

$$bias = \frac{1}{N}\sum_{i=1}^{N} P_i - M_i \tag{2}$$

$$R = \frac{\sum_{i=1}^{N}(P_i - \bar{P})(M_i - \bar{M})}{\sqrt{[\sum_{i=1}^{N}(P_i - \bar{P})^2][\sum_{i=1}^{N}(M_i - \bar{M})^2]}} \tag{3}$$

where N is the record length, M_i is the measured data, P_i is the modeled data, and bar accents are time averages.

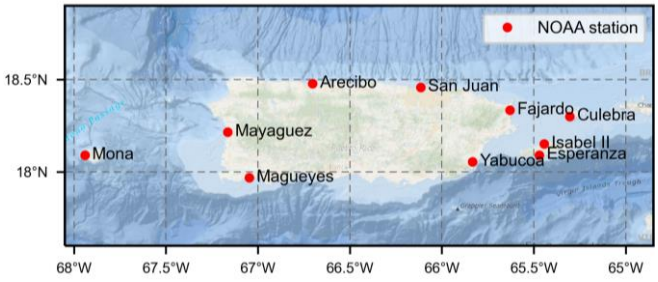

Fig. 1. Puerto Rico NOAA buoy locations around.

For tides and ocean currents, the available in-stream power per unit area, or theoretical power density, is computed as

$$P = \frac{1}{2}\rho_w v^3 \tag{4}$$

where ρ_w is the density of water and v is the magnitude of the stream velocity [5].

The power density for OTEC systems, or power per unit of upwelled cold water, is estimated as

$$\frac{P}{Q} = \frac{\rho_w C_p E_{TG}(\Delta T)^2(1 - PL)}{8(273 + SST)} \tag{5}$$

where P is the thermal power, Q is the deep seawater flowrate, ρ_w is the average density of water, C_p is the specific heat of water, E_{TG} is the turbogenerator efficiency, ΔT is the temperature differential between the sea surface temperature, SST, and the environmental temperature at the depth of cold water intake, and PL are the energy losses due to pumping [6]. In this study, we set E_{TG} as 1 and PL as 0, to obtain a technology agnostic.

III. RESULTS

A. Model performance

The accuracy of the ADCIRC model was evaluated using NOAA in-situ measurements. The computed error metrics shown in Table II indicate a high model skill in predicting the tidal range. Time-series comparisons also showed that the model is effective in simulating the spring-neap tidal cycle.

TABLE II
ERROR STATISTICS AT NOAA WATER LEVEL STATIONS

Station ID	Quantity	RMSE (m)	Bias (m)	R
9855371	San Juan	0.040	0.000	0.97
9757809	Arecibo	0.039	0.001	0.97
9759394	Mayaguez	0.034	0.001	0.96
9759110	Magueyes	0.032	0.000	0.91
9754228	Yabucoa	0.028	0.001	0.94
9753216	Fajardo	0.026	0.000	0.98
9759938	Mona	0.029	-0.001	0.93
9752235	Culebra	0.023	0.000	0.98
9752695	Esperanza	0.031	0.001	0.92
9752619	Isabel Segunda	0.024	0.001	0.98

All measured time-series retrieved include N = 745 data points.

The AmSeas and HYCOM models are independently calibrated, but for use in this study they were compared against historical records to verify their accuracy. AmSeas ocean currents were validated against HF radar imagery, and HYCOM ocean temperatures were validated against satellite imagery from Multi-scale Ultra-high Resolution analysis of Sea Surface Temperature (MURSST) and ARGO floats. Both models were shown to be consistent with the historical datasets.

B. Power density estimates and hotspot identification

Fig. 2 shows the average tidal power density, and probability of exceeding tidal currents of 30 cm/s as a sample threshold. Our study showed that although tidal stream resources around Puerto Rico are low, some hotspots exist around the main island with mean tidal current speed exceeding 50 cm/s for more than 50% of the time, including the northwestern edge of Tourmaline Reef off the western coast of Puerto Rico, and between Vieques island and the mainland off to the east.

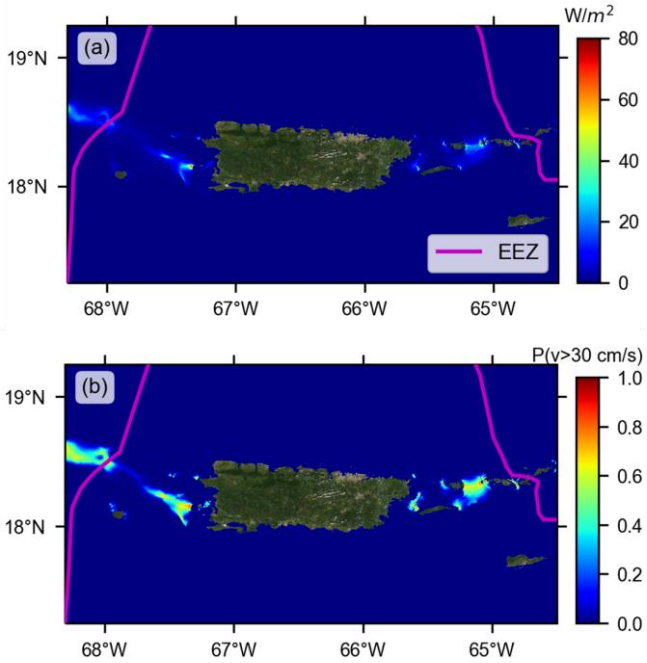

Fig. 2. (a) Average tidal power density, and (b) probability of exceeding speeds of 30 cm/s. U.S. Economic Exclusive Zone (EEZ) is shown in magenta.

Fig. 3 shows the average ocean current power density, and probability of exceeding a sample threshold of 30 cm/s. For ocean currents, substantial resource is present in the southern area of Tourmaline Reef where ocean currents exceed 50 cm/s over 55% of the time, while closer to St. Thomas, U.S. Virgin Islands, currents exceed 50 cm/s over 35% of time.

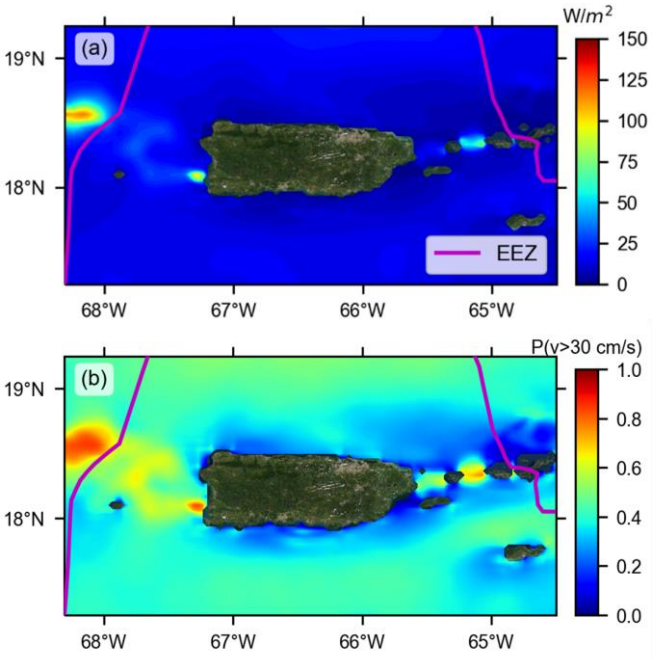

Fig. 3. (a) Average ocean current power density, and (b) probability of exceeding speeds of 30 cm/s.

The thermal resource potential is assessed based on the availability of a minimal thermal gradient of 20°C between the warm sea surface and a cold water collection depth typically needed for OTEC operation [7]. Fig. 4 shows seasonal distributions of depths at which this criterion is met, with regions that do not ever meet it shown in white.

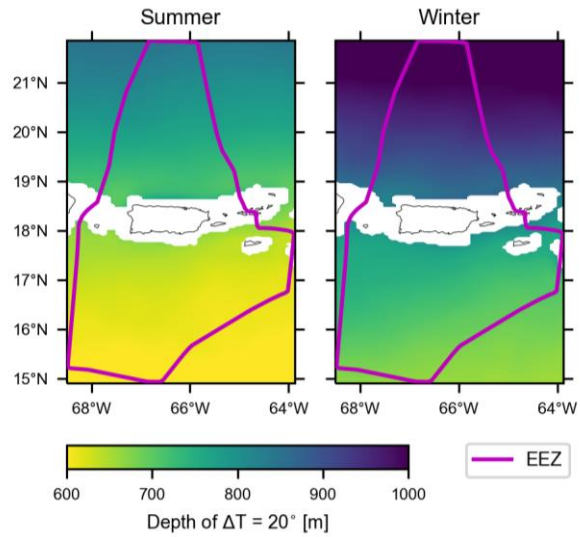

Fig. 4. Summer and winter distributions of depths where the average thermal gradient is 20°C.

The critical operational depths for OTEC operation near Puerto Rico show clear seasonal and geographic variability. This is also reflected in the distribution of thermal gradients at fixed depth layers (Fig. 5).

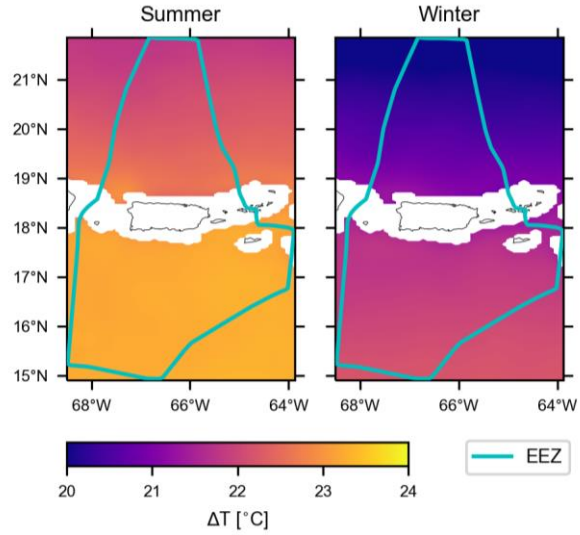

Fig. 5. Summer and winter thermal gradient distributions between the sea surface and a sample depth of 1 km.

The OTEC power density for systems pumping cold water from a sample depth of 1 km is shown in Fig. 6. Overall, there is greater energy harvesting potential south of Puerto Rico in the Caribbean Sea than to the north in the Atlantic Ocean. While a high-level average analysis like this one is useful for obtaining an approximate estimate of the power density and identifying the relative geographic potential of OTEC at a given depth, it overrepresents the available power because the averaging calculations include times when the thermal gradients fall below the critical threshold of 20°C at which a typical OTEC plant would generate no power.

For a more in-depth analysis, two locations are selected to the north and south sides of Puerto Rico for a temporal analysis (blue circles in Fig. 6). These locations were chosen for their proximity to the main island which would reduce installation and maintenance cost for potential OTEC plants, and to contrast the thermal resource in each basin.

Fig. 7 and Fig. 8 show histograms and exceedance probability graphs of OTEC power density estimated from sea water temperature time-series corresponding to a cold-water intake depth of 800 m. The chosen depth illustrates the conditions when a plant would not achieve year-round operation. OTEC plants at either location would produce 700 to 1,000 kW per m³/s of power but would only be operational (i.e., $\Delta T \geq 20°C$) 70% and 90% of the time at the northern and southern stations, respectively.

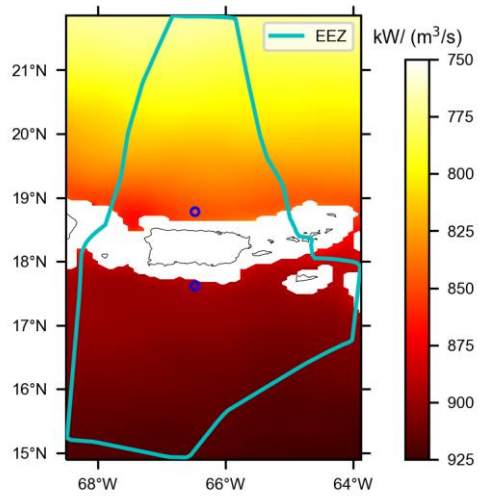

Fig. 6. OTEC power density at a sample depth of 1 km based on average values of SST and ΔT. The blue circles are sample locations selected for a temporal analysis.

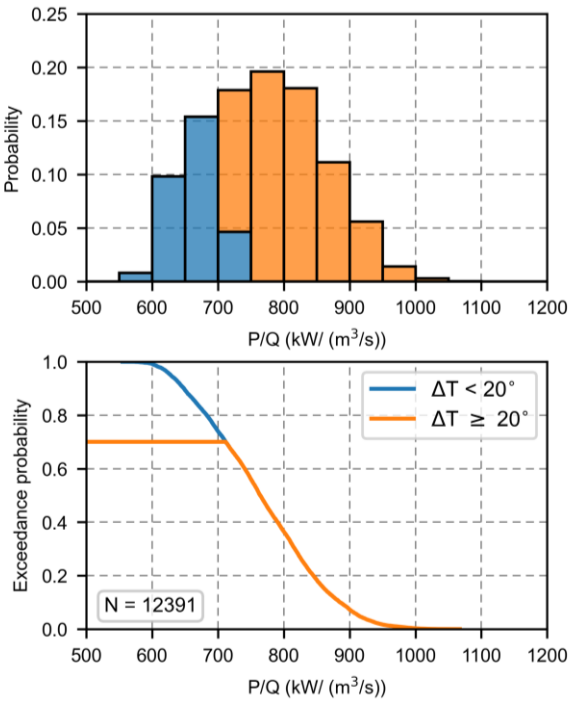

Fig. 7. OTEC power density histogram and exceedance probability north of Puerto Rico (18.8°N,66.5°W) for a cold-water depth of 800 m.

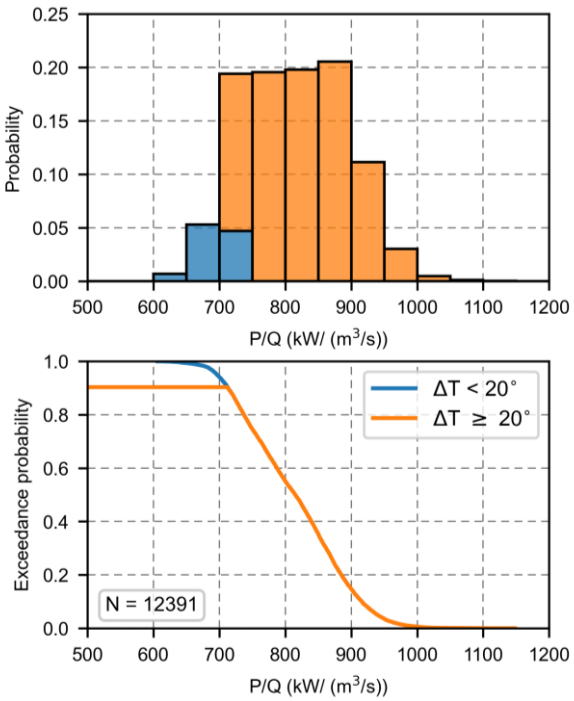

Fig. 8. OTEC power density histogram and exceedance probability south of Puerto Rico (17.6°N,66.5°W) for a cold-water depth of 800 m.

IV. Discussion & Conclusion

In this study, we analyzed the viability of using tidal streams, ocean currents, and ocean thermal resources to supply power for Puerto Rico based on various hydrodynamic models. The energy availability of tidal and thermal resources near Vieques island could augment the resiliency of Vieques, which presently sources their electricity from the main island of Puerto Rico and is vulnerable to power shutdowns when coastal hazards (e.g., tropical storms and hurricanes) impact the region. Significant tidal and ocean current power sources were identified near Tourmaline Reef off the western coast of the main island, which could have various applications from community coastal resiliency to supporting coastal activities such as aquaculture. Additional locally strong tidal streams (exceeding 30 cm/s) where identified in small channels east of the main island, but only significant enough to power small scale applications. OTEC is the most promising electricity generation source near the northern and southern regions of Puerto Rico.

The thermal resource was analyzed further by focusing on point locations about 1 km north and south from the coast of Puerto Rico, showing promising results for OTEC operation. The temporal analysis at both locations, showed a more realistic estimate of potential power production by an OTEC plant. Future work will expand on this approach for a combined geospatial and temporal analysis to optimize the depth of cold-water intake pipes.

REFERENCES

[1] U.S. Department of Energy, "Puerto Rico Grid Resilience and Transitions to 100% Renewable Energy Study (PR100)," Energy.gov, 2022. https://www.energy.gov/gdo/puerto-rico-grid-resilience-and-transitions-100-renewable-energy-study-pr100 (accessed Dec. 07, 2022).

[2] B. R. Joyce et al., "U.S. IOOS Coastal and Ocean Modeling Testbed: Hurricane-Induced Winds, Waves, and Surge for Deep Ocean, Reef-Fringed Islands in the Caribbean," J. Geophys. Res.: Oceans, vol. 124, no. 4, pp. 2876–2907, 2019, doi: 10.1029/2018JC014687.

[3] "FNMOC Regional Navy Coastal Ocean Model," National Centers for Environmental Information (NCEI), Sep. 2022. https://www.ncei.noaa.gov/products/weather-climate-models/fnmoc-regional-navy-coastal-ocean (accessed Dec. 09, 2022).

[4] HYCOM Consortium for Data Assimilative Modeling, "HYCOM Sata Server." https://www.hycom.org/dataserver (accessed Dec. 12, 2022).

[5] Georgia Institute of Technology, "Assessment of Energy Production Potential from Tidal Streams in the United States," Georgia Institute of Technology, Atlanta, GA (United States), United States, Final Project Report DE-FG36-08GO18174, Jun. 2011. doi: 10.2172/1219367.

[6] National Research Council, An Evaluation of the U.S. Department of Energy's Marine and Hydrokinetic Resource Assessments. Washington, D.C.: The National Academies Press, 2013. doi: 10.17226/18278.

[7] L. A. Vega, "Oceanocean/oceanicThermal Energy Conversionocean/oceanicthermal energy conversion (OTEC)," in Encyclopedia of Sustainability Science and Technology, R. A. Meyers, Ed., New York, NY: Springer, 2012, pp. 7296–7328. doi: 10.1007/978-1-4419-0851-3_695.